Anatomical Science International (2023) 98:309–317
https://doi.org/10.1007/s12565-023-00703-z

METHOD PAPER

Revealing the Underlying Morphology: Challenging Reductionism Through 3D Visualization for Future Anatomy

Three-dimensional mouse cochlea imaging based on the modified Sca/eS using confocal microscopy

Shinji Urata[1] · **Shigeo Okabe**[2]

Received: 15 December 2022 / Accepted: 13 January 2023 / Published online: 11 February 2023

Abstract

The three-dimensional stria vascularis (SV) and cochlear blood vessel structure is essential for inner ear function. Here, modified Sca/eS, a sorbitol-based optical-clearing method, was reported to visualize SV and vascular structure in the intact mouse cochlea. Cochlear macrophages as well as perivascular-resident macrophage-like melanocytes were detected as GFP-positive cells of the CX3CR1$^{+/GFP}$ mice. This study's method was effective in elucidating inner ear function under both physiological and pathological conditions.

Keywords Stria vascularis · Cochlea · Optical tissue clearing · Sca*l*eS · Macrophage

Introduction

The cochlea is a sound-receptive sensory organ located in the temporal bone. Sound vibrations to the tympanic membrane are transmitted to the inner ear through the middle ear ossicles (Fig. 1A). The sensory epithelium formed by hair cells convert sound stimuli into electrical signals and the signal is transferred to the auditory cortex. Lymph fluid generated by nonsensory epithelium cells fills the cochlea and regulates cochlear function (Fig. 1B). Endolymph is produced in the stria vascularis (SV) in the bony cochlear wall (Tasaki and Spyropoulos 1959). Stratified epithelium in the SV consists of three cell types: marginal, intermediate, and basal (Fig. 1C). K^+ transporter expressed on the marginal cells is essential in maintaining endolymphatic high potential (Nin et al. 2008). Intermediate cells are pigment-containing cells classified as a unique macrophage type, such as perivascular-resident macrophage-like melanocyte (PVM/Ms) (Zhang et al. 2012). Gap junctions connect basal cells in the SV to the fibrocytes in the spiral ligament (Kikuchi et al. 1995). The previous SV studies have elucidated cochlear function using primarily electrophysiological analysis. The SV cell group ultrastructure has been visualized using an electron microscopy. However, wide-field imaging of the lateral cochlear wall, including SV, spiral ligament, and the bony cochlear wall, has not been performed because of its anatomic location. The cochlea is covered with bone and has a hollow structure lined with a membrane. For physiological analysis of both sensory and nonsensory epithelium cells, traditional histology and immunohistochemistry should be optimized for sample sectioning. Alternatively, whole-mount surface preparation has been performed (Mizushima et al. 2017; Fujimoto et al. 2017).

Optical tissue clearing enables structural visualization and molecular information acquisition from large-volume tissues. Optical tissue-clearing methods combined with light-sheet or two-photon microscopy have enabled structural acquisition of the rodent's sensory epithelium (Toulemonde et al. 2022; Hutson et al. 2021; Tinne et al. 2017; Brody et al. 2020; Moatti et al. 2022, 2020; Nolte et al. 2017; Risoud et al. 2017; Malfeld et al. 2021; Keppeler et al. 2021). However, an optimized method using confocal microscopy to analyze the intact rodent's cochlea has not yet been developed (Wrzeszcz et al. 2013; MacDonald and Rubel 2008, 2010).

Lead contact: Shinji Urata.

✉ Shinji Urata
surata@m.u-tokyo.ac.jp

[1] Department of Otolaryngology, Graduate School of Medicine, University of Tokyo, Tokyo 113-0033, Japan

[2] Department of Cellular Neurobiology, Graduate School of Medicine, the University of Tokyo, Tokyo, Japan

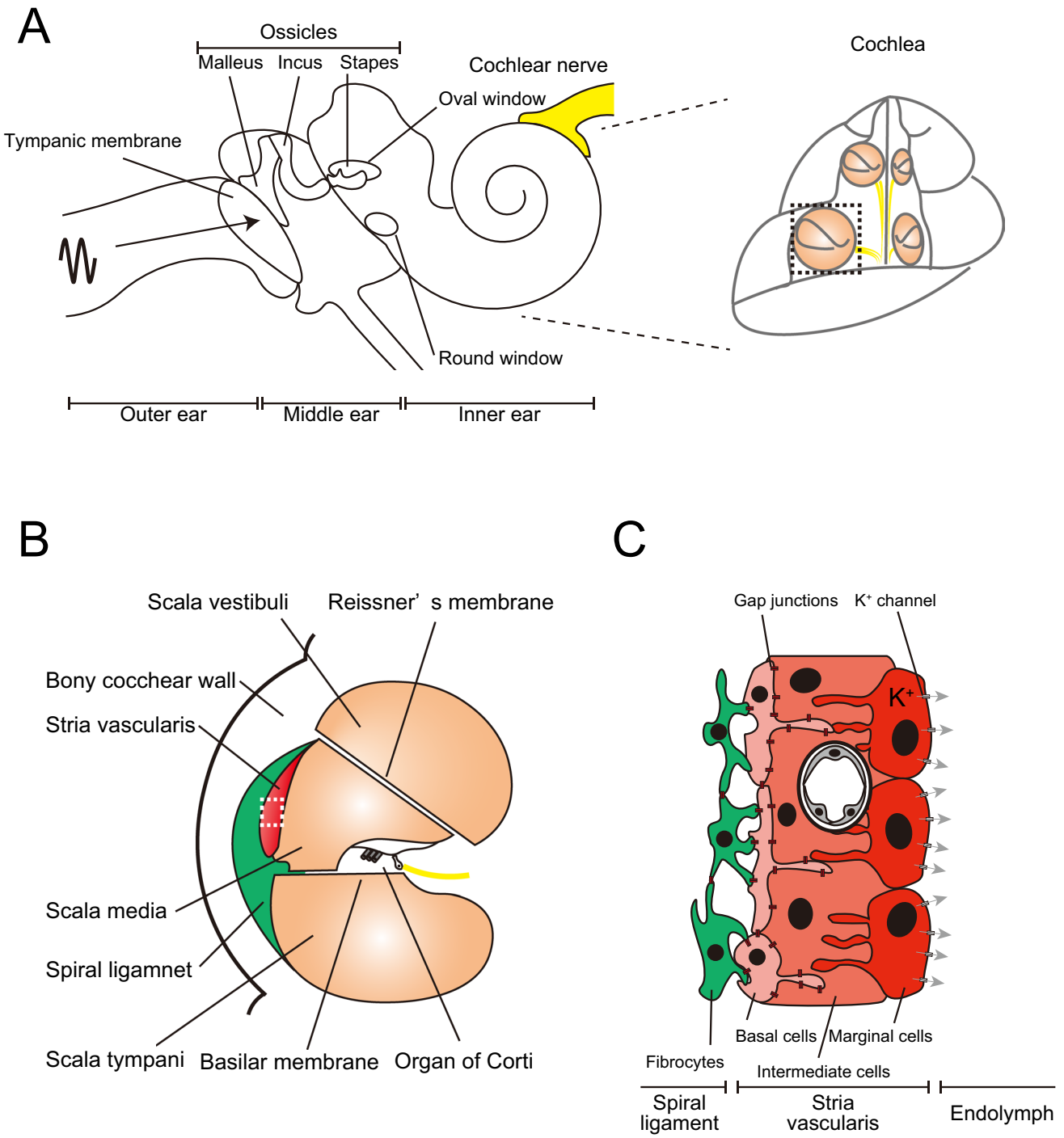

Fig. 1 Auditory pathway anatomy. **A** Sound wave is transferred to the tympanic membrane. Stimulation is amplified by three tiny bones ("ossicles") and transferred to the inner ear through the oval window to the round window in the cochlea. Stimulation vibrates the basilar membrane in the cochlear duct (pale orange) and electrical stimuli converted in the Corti organ are transferred to the brain through the cochlear nerve (yellow). **B** Anatomical structures of the cochlear duct (black dashed squared in **A**). Membrane structures, including cochlear duct (pale orange), stria vascularis (red), spiral ligament (green), organ of Corti, and cochlear nerve (yellow), are covered with bone. **C** A schematic compartmental model of the lateral cochlear wall (white dashed squared in **B**). Stria vascularis (SV) consists of three cellular components: marginal (red), intermediate (orange), and basal (pink). Potassium-regulating channels are located in the marginal cells (arrows, flow of K^+ ions). Gap junctions are expressed in the basal cells and connect to the intermediate cells and fibrocytes in the spiral ligament (green)

In this study, modified Sca/eS was described to enables us to visualize the SV structures and blood vessels and the immune cells, such as cochlea macrophages and PVM/Ms, in the intact mouse cochlea.

Materials and methods

Sample preparation

Mouse husbandry, anesthesia, and euthanasia conformed to related regulations of the government and the institutional guidelines. All animal studies are reviewed and approved by the Animal Care and Use Committee of the Graduate School of Medicine, the University of Tokyo. This study used male and female 8–12 week-old C57BL/6 or CX3CR1 mutant mice (Steffen et al. 2000). The mice's CX3CR1 was replaced with GFP. Therefore, heterozygous CX3CR1$^{+/GFP}$ mice were used on the C57BL/6 background. CX3CR1 is the specific receptor for the chemokine fractalkine (CX3CL1) and expressed in monocytes, macrophages, microglia, subsets of NK and dendritic cells, and active T cells (Steffen et al. 2000). In the mouse cochlea, CX3CR1 is expressed in resident macrophages, perivascular macrophages, and infiltrating monocytes (Hough et al. 2022). Animals were anesthetized with a ketamine−xylazine mix (ketamine, 100 mg/kg; xylazine, 20 mg/kg). After euthanasia, mice were perfused transcardially with 4% paraformaldehyde (PFA) in phosphate-buffered saline (PBS). Temporal bones were extracted and the samples were incubated in 4% PFA in PBS at 4 °C for 12 h. Decalcification was performed by incubating samples for 72 h in 500 mM EDTA in PBS at 37 °C and terminated by washing samples several times with PBS. Subsequently, the inner ear was dissected from the temporal bone under a stereo microscope.

Transcardial vascular staining

Before transcardial perfusion−fixation, anesthetized mice were injected with 50 µl of 1 mg/ml *Lycopersicon esculentum* lectin conjugated to DyLight649 (DL-1178, Vector-Labs) from the tail vein. After 5 min, mice were transcardially perfused with 4% PFA with PBS (Battistella et al. 2021).

Labeling with small molecules

Samples were washed with PBS containing 0.1% Triton X-100 for 30 min with continuous rocking at 40 rpm. Subsequently, samples were incubated for 2 h in a solution containing 100 nM small molecules (rhodamine-conjugated phalloidin, Molecular Probes) with appropriate dilutions at 37 °C. Finally, small molecules were removed by washing for 1 h with PBS containing 0.1% Triton X-100, with continuous rocking at 40 rpm.

Refractive index (RI) matching

Modified Sca/eS were adopted, as a tissue-clearing method, according to the previous report (Urata et al. 2019a, b). Briefly, samples were washed three times by PBS containing 0.1% Triton X-100 for 10 min after small molecules staining. Samples were placed in a chamber with the RI matching solution, covered by a coverslip, and imaged by a confocal microscope. RI matching solution consisted of 4 M urea, 60% (w/v) D-sorbitol, and 0.1% (w/v) Triton X-100 in PBS (pH 7.1).

Image acquisition

Fluorescent images were performed on a confocal microscope system (A1R, Nikon, Japan) with a 20× water immersion objective lens (NA = 0.95). GFP, rhodamine phalloidin, and DyLight649 were excited with 488, 564, and 635 nm, respectively. A chamber containing the sample was filled with the RI matching solution, covered by a glass coverslip, and placed under objective lens. Single horizontal image sizes were set to 512×512 with pixel sizes of 1.23×1.23 µm and z-spacing of 2 µm. The ImageJ software (National Institute of Health) was used to perform image processing and Imaris (Bitplane) and NIS-Element AR (Version 4.51, Nikon) was used to perform three-dimensional rotation.

Results

F-actin-labeled cochlea was imaged from the apical to the basal portion along the cochlear modiolus. Since F-actin protein is a major cytoskeleton component, all cochlear cells can be identified as rhodamine phalloidin-positive cells. Blood vessels toward the bony cochlear wall (arrows in Fig. 2A) and Reissner's membrane structure (Fig. 2B) were observed. Borders of the lateral wall components were apparent (Fig. 2C). The three-dimensional image was reconstructed based on the two-dimensional images (Fig. 2F). The SV and spiral ligament's three-dimensional structure were visualized, thus the SV and spiral ligament borders were recognized (Fig. 2F, G).

Then, the vascular structure in the cochlea was investigated by injecting the *Lycopersicon esculentum* lectin conjugated to DyLight649 under anesthesia (Supplemental Movie 1). The stapedial artery, which passes through the stapes (arrow in Fig. 3A), can be identified, as well as cochlear blood vessels (Fig. 3A). In addition, the image along the modiolus enabled us to visualize the radiating arterioles (arrow in Fig. 3B) from the main cochlear artery in the

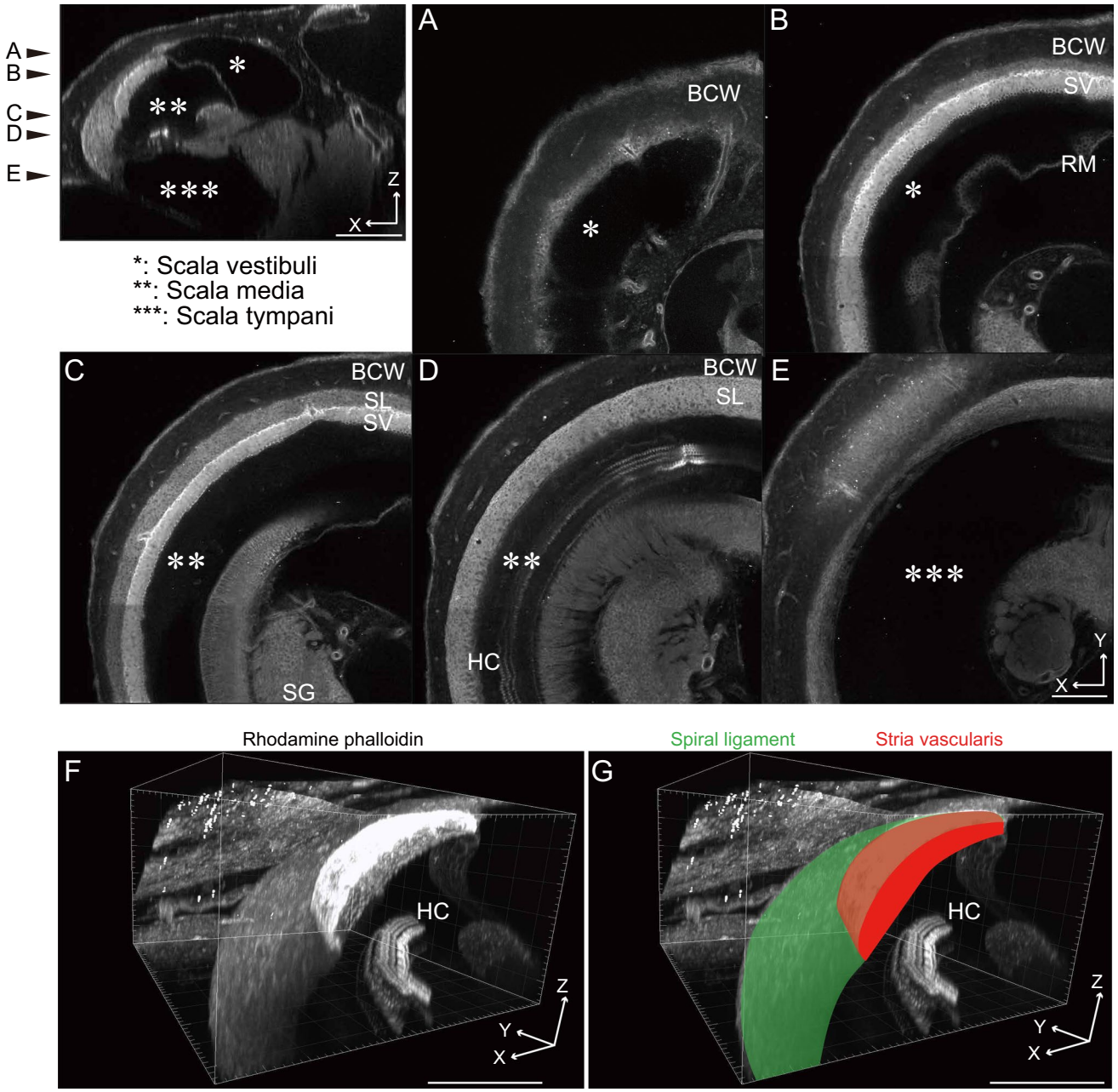

Fig. 2 Three-dimensional structure of cytoskeleton labeled with F-actin. The cochlear duct cross-section is shown in the left top panel. Scala vestibule (single asterisk), scala media (double asterisk), and scala tympani (triple asterisk) are visualized in the cochlear duct. The two-dimensional images at several planes (**A**–**E**) are shown. The three-dimensional lateral cochlear wall is reconstructed and the stria vascularis (red) and spiral ligament (green) are clearly identified (**F**, **G**). *BCW* bony cochlear wall, *HC* hair cell, *RM* Reissner's membrane, *SG* spiral ganglion, *SL* spiral ligament, *SV* stria vascularis. Scale bar, 200 µm

modiolus (single asterisk in Fig. 3B) to the vessels in the lateral wall (double asterisk in Fig. 3B) and spiral vessels (triple asterisk in Fig. 3B).

Macrophages were widely present in the cochlea. Nevertheless, the role of macrophages is still enigmatic (Hough et al. 2022). Its activation is characterized by changes in macrophage morphology, mediator expression, and distribution. Ramified macrophages have long dendritic processes with small cell bodies. In contrast, amoeboid macrophages are flat-shaped. GFP-positive cells were identified as macrophages (Fig. 4, Supplemental Movie 2). Ramified, amoeboid, and dendritic-to-amoeboid macrophages were located in the SV (arrows in Fig. 4B), basilar membrane (arrows in Fig. 4D), and bony cochlear wall on the scala vestibuli (arrows in Fig. 4A), respectively. Ramified macrophages were aligned to SV

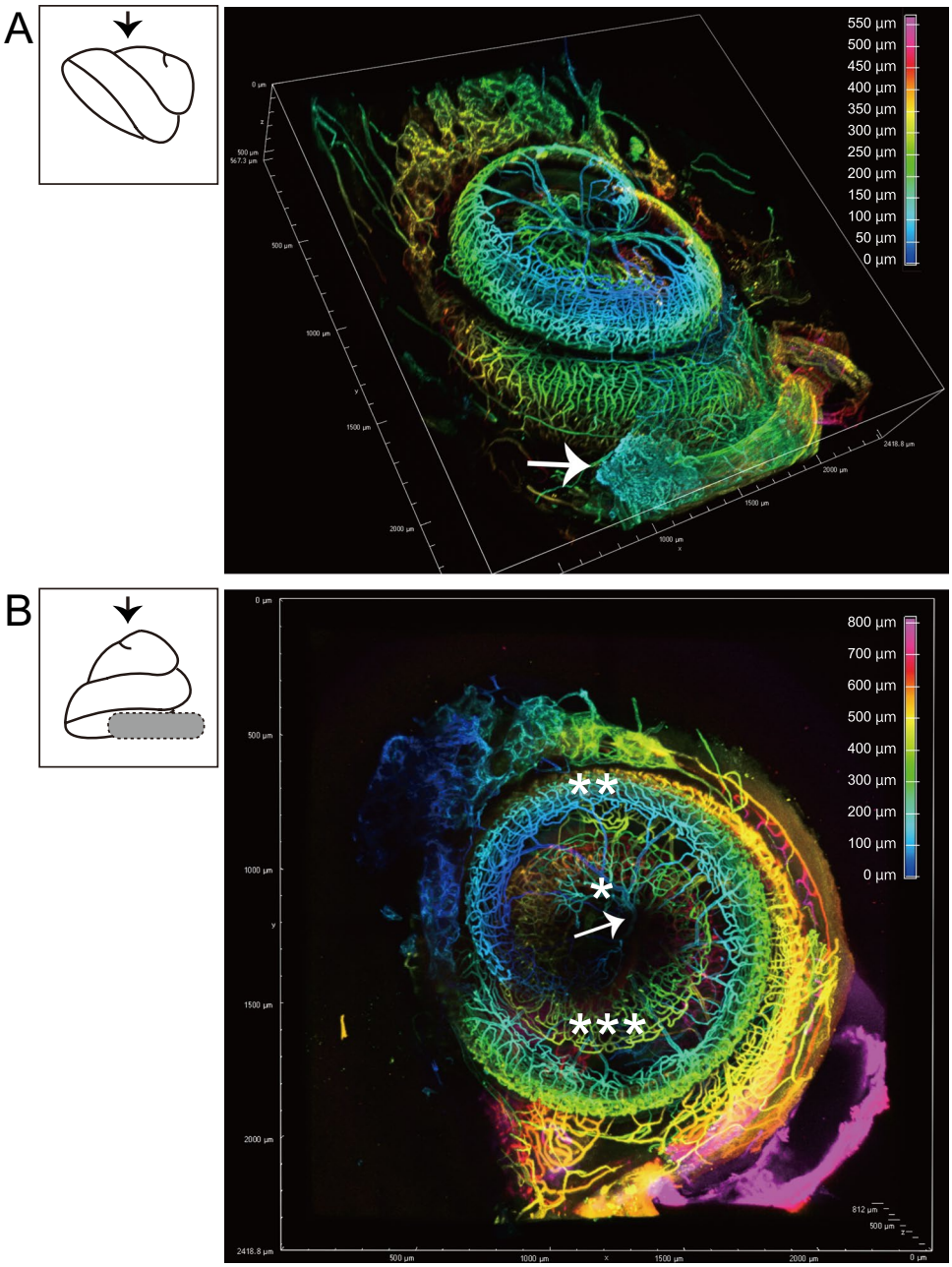

Fig. 3 Vasculature of the mouse cochlea labeled by lectin. **A** The cochlea is placed on the glass slide. Images are acquired in parallel with the bony cochlear wall of the surface side (black arrow). Cochlear vasculature is widely visualized. Stapedial vessels on the surface of the cochlear bony wall are also observed (white arrow). The color bar shows the depth from the surface plane. **B** A pedestal (gray ellipse) is placed so that the axis of the cochlear center is aligned perpendicular to the glass slide. Images are acquired along the modiolus from the apical portion (black arrow). Radiating arterioles (white arrow), main cochlear artery (single asterisk), lateral wall vessels (double asterisk), and spiral vessels (triple asterisk) are visualized. The color bar shows the depth from the surface plane

blood vessels. The perivascular macrophage is located in the intermediate layer because they were above the marginal cell layer (single asterisk in Fig. 4B). Additionally, macrophages were identified on Reissner's membrane and a lectin-labeled blood vessel in the bony cochlear wall was visualized (arrows in Fig. 4C). Various macrophage types seemed to closely occupy the lower part of the spiral ligament (asterisk in Fig. 4D) compared to those of the upper (double asterisk in Fig. 4B) and middle (asterisk in Fig. 4C) parts. The cochlear macrophage shape in the spiral limbus was dendritic-to-amoeboid and located adjacent to spiral vessels (single asterisk in Fig. 4E).

Discussion

The optical tissue-clearing method, modified Sca/eS, was demonstrated to enable structural visualization of the intact mouse cochlea's SV and blood vessels. Furthermore, confocal microscopy could widely observe GFP expressed in mouse cochlea macrophages.

A complete understanding of the cochlear function relies on an accurate description of the three-dimensional cochlear structure. The components required for sound perception are covered by the temporal bone and cochlear

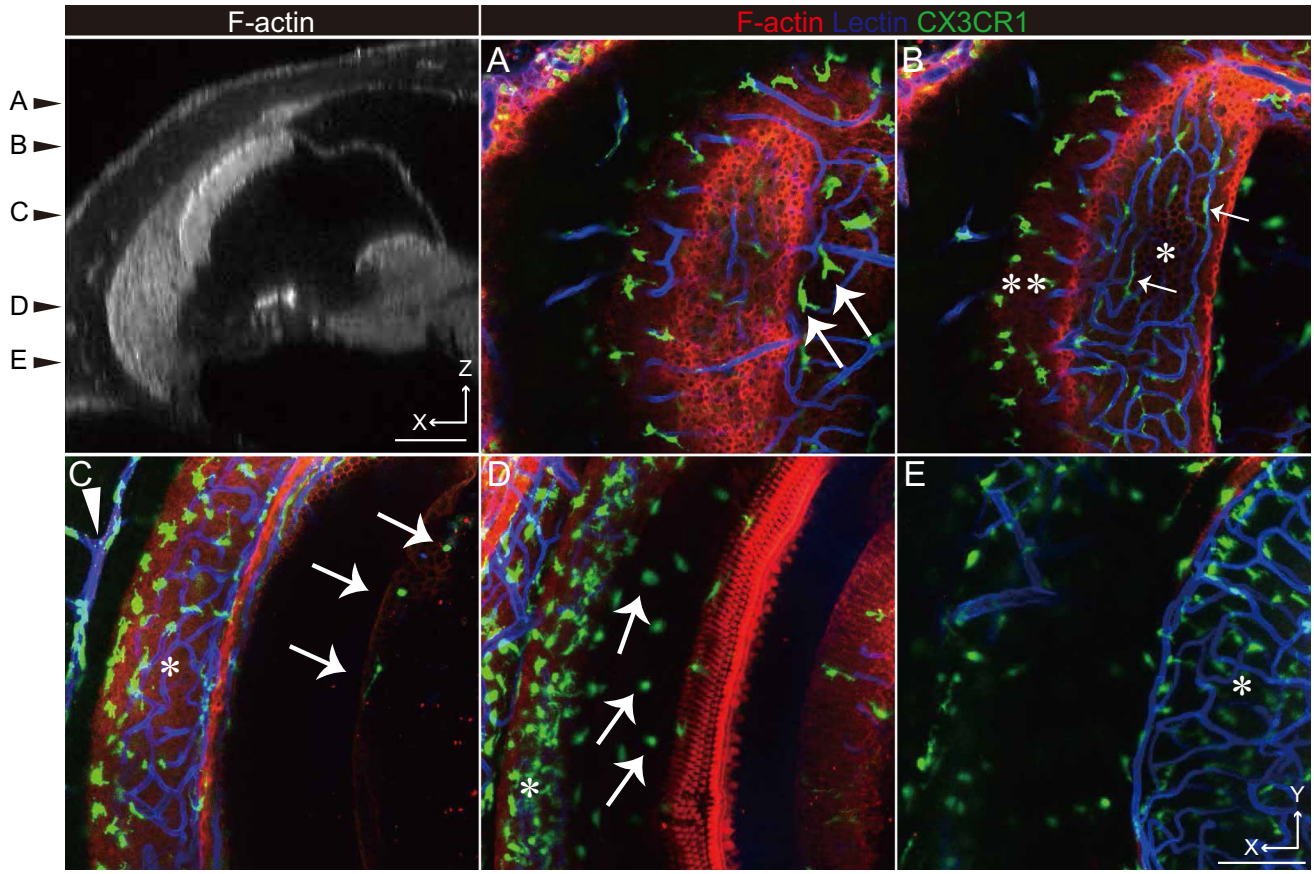

Fig. 4 Macrophage distribution in the cochlea. The cochlear duct cross-section labeled with F-actin is shown in the left top panel. The two-dimensional cochlear images of the CX3CR1 mouse labeled with rhodamine phalloidin (red) and lectin (blue) at several planes (**A**–**E**) are shown. GFP is widely expressed in the cochlea (**A**–**E**) and various macrophage shapes, dendritic-to-amoeboid (arrows in **A**, **E**), ramified (arrows in **B**), and amoeboid (arrows in **D**), are expressed in the stria vascularis (asterisk in **B**), spiral ligament (double asterisk in **B**, single asterisk in **D**), spiral limbus (single asterisk in **E**), and cochlear bony wall (arrowhead in **C**). Scale bar, 100 µm

bony wall. Therefore, traditional protocols, such as thin sectioning and whole-mount surface preparation, have been performed to understand cochlear morphology. Those protocols are rigidly established and highly reproducible. However, three-dimensional cellular distribution in the SV and Reissner's membrane is still an enigma because the field of view is highly restricted in these conventional techniques.

The cochlea's F-actin-stained cellular structure was described using the modified Sca/eS (Fig. 2). This method enabled three-dimensional structural visualization of the cochlea. The entire volumes of the organ of Corti, SV, and spiral ligament could be measured by tracing the targeted area (Supplementary Fig. 1). This method is likely to be an alternative tool for researching Meniere's disease. Based on the clinical study with high-resolution contrast-enhanced magnetic resonance imaging, endolymphatic hydrops of the scala media (double asterisk in Fig. 2) have been considered the primary pathology of Meniere's disease (Niyazov et al. 2001). Furthermore, in vivo and in vitro animal studies support this hypothesis (Egami et al. 2013; Kakigi et al. 2020). Nevertheless, a complete scala media survey has been difficult because the membrane structure, such as Reissner's membrane and basilar membrane, are transformed due to fixation and/or dissection, as well as image acquisition plane perpendicular to the modiolus.

Recently, in vivo live cochlear imaging using two-photon microscopy revealed that the gentamicin transporter, expressed in the SV and involved in the blood−labyrinthine−barrier function, protects against gentamicin-induced hearing loss, which causes drug-induced hearing loss in a significant patient population (Kim and Ricci 2022). Including drug-induced hearing loss, SV is an important component because sound exposure, which causes noise-induced hearing loss, decreases SV blood flow (Burwood et al. 2020). Previous reports have revealed cochlear blood vessel details. However, complete morphology of intact cochlea has not been acquired (Nomura and Hiraide 1968; Axelsson 1988; Jiang et al. 2019). In recent advancements in optical tissue clearing, the intact mouse brain's blood vessel

structure cleared by CLARITY (Giovanna et al. 2018) and 3DISCO (Lugo-Hernandez et al. 2017) were visualized. Furthermore, unbiased and scalable vasculature quantification of cleared mouse brains was developed using machine learning (Todorov et al. 2020). Visualization of cochlear blood vessels labeled with lectin (Fig. 3, Supplemental Movie 1) was demonstrated. The method will quantify the cochlea's angioarchitecture under various conditions, such as age-, noise-, and drug-induced hearing loss.

Accumulating information about macrophages in the cochlea is essential to understand the inner ear's immune system. Macrophages are pervasive in the steady-state cochlea: SV, spiral ligament, spiral ganglion, and basilar membrane (Hirose et al. 2005). Macrophages in the cochlea responds against stresses derived from noise exposure and ototoxic drug and its morphology is transformed by noise-, drug- and age-induced hearing loss (Frye et al. 2017). In animal studies, macrophages in Reissner's membrane have been derived only under stressed conditions (Sautter et al. 2006). However, macrophages in Reissner's membrane were observed in humans suffering from life-threatening posterior cranial fossa meningioma (Liu et al. 2021). Recently, CX3CR1-positive cells were recognized in Reissner's membrane of the quiescent mouse cochlea by using two-photon microscopy (Bae et al. 2021). This study's result is consistent with this report (arrows in Fig. 4C, Supplementary Movie 2).

Previous reports have revealed two macrophage types in the lateral cochlear wall: cochlear macrophage in the spiral ligament and PVM/Ms in the SV (Fujioka et al. 2014). PVM/Ms is a melanin-positive macrophage and maintains blood−labyrinthine barrier integrity (Zhang et al. 2012). Moreover, based on their location and morphology, previous reports proposed that PVM/Ms can be classified as pericytes and intermediate cells. PVM/Ms are macrophages bearing dendritic processes located adjacent strial capillaries (Shi 2010; Neng et al. 2013). All CX3CR1-positive cells in the intermediate cell layer were found on blood vessels (arrows in Fig. 4B, Supplementary Movie 2).

The imaging depth of conventional confocal imaging is limited to approximately 100 µm, prohibiting wide-field imaging with a single-cell resolution of the cochlea (Nwaneshiudu et al. 2012). Optical access to cell properties is an effective tool for cell biology. Various optical tissue-clearing methods, including Sca/e (Hama et al. 2011), CLARITY (Chung and Deisseroth 2013), CUBIC (Susaki et al. 2014), and 3DISCO (Ertürk et al. 2012), have enabled mouse brain structural and molecular information acquisition. Recently, other advanced techniques optimized for wide-field imaging (Susaki et al. 2015; Murakami et al. 2018) and hard tissue containing extracellular matrix (Greenbaum et al. 2017; Wang et al. 2019; Pan et al. 2016) were reported. Using two-photon microscopy, both organic- (MSBB (Hutson et al. 2021): methyl-salicylate and benzyl benzoate, iDISCO (Moatti et al. 2020)) and hydrophilic-solution-based clearing methods (Urata et al. 2019b) enabled us to visualize gerbil (Hutson et al. 2021), porcine (Moatti et al. 2020), and mouse (Urata et al. 2019b) sensory epithelium cells in the cochlea. Even though optimized MSBB is an organic-solution-based clearing method, confocal microscopy is insufficient to visualize all components of intact rodent's cochlea (Risoud et al. 2017; Malfeld et al. 2021; Wrzeszcz et al. 2013; MacDonald and Rubel 2008, 2010).

The imaging method described in this study has several limitations. GFP and *Lycopersicon esculentum* lectin fluorescence conjugated to DyLight649 were sufficient for detection by single-photon excitation. However, rhodamine phalloidin fluorescence was weaker and laser intensity adjustment was necessary for deep tissue imaging. Furthermore, deep inside the cochlea, fine structures (stereocilia) found on hair cell surfaces were not visualized. Improvement in the labeling method may overcome this difficulty, but the current immunostaining techniques combined with conventional confocal microscopy were insufficient. Therefore, a 2-way imaging protocol was developed according to the previous reports (Supplementary Fig. 2). The method supported image acquisition of mouse cochlea all along its imaging depth. Recently, gerbil (Toulemonde et al. 2022) and guinea pig (Brody et al. 2020) sensory epithelium have been visualized by nontoxic organic compound ethyl cinnamate (ECi) with two-photon microscopy. Refractive index (RI) of ECi (1.558) is similar to DBE (1.562) which was used as the mounting solution of organic-solution-based-clearing method. Therefore, ECi seems to be useful for intact cochlear imaging by confocal microscopy.

Supplementary Information The online version contains supplementary material available at https://doi.org/10.1007/s12565-023-00703-z.

Funding Open access funding provided by The University of Tokyo.

Declarations

Conflict of interest The authors declare that they have no conflict of interest.

References

Axelsson A (1988) Comparative anatomy of cochlear blood vessels. Am J Otolaryngol 9(6):278–290. https://doi.org/10.1016/S0196-0709(88)80036-X

Bae SH, Kwak SH, Yoo JE et al (2021) Three-dimensional distribution of cochlear macrophages in the lateral wall of cleared cochlea. Clin Exp Otorhinolaryngol 14(2):179–184. https://doi.org/10.21053/ceo.2020.00395

Battistella R, Kritsilis M, Matuskova H et al (2021) Not all lectins are equally suitable for labeling rodent vasculature. Int J Mol Sci 22(21):11554

Brody KM, Hampson AJ, Cho H, Johnson P, O'Leary SJ (2020) A new method for three-dimensional immunofluorescence study of the cochlea. Hear Res 392:107956

Burwood GWS, Dziennis S, Wilson T et al (2020) The mechanoelectrical transducer channel is not required for regulation of cochlear blood flow during loud sound exposure in mice. Sci Rep 10(1):9229. https://doi.org/10.1038/s41598-020-66192-6

Chung K, Deisseroth K (2013) CLARITY for mapping the nervous system. Nat Methods 10(6):508–513

Di Giovanna AP, Tibo A, Silvestri L et al (2018) Whole-brain vasculature reconstruction at the single capillary level. Sci Rep 8(1):12573. https://doi.org/10.1038/s41598-018-30533-3

Egami N, Kakigi A, Sakamoto T, Takeda T, Hyodo M, Yamasoba T (2013) Morphological and functional changes in a new animal model of Ménière's disease. Lab Investig 93(9):1001–1011. https://doi.org/10.1038/labinvest.2013.91

Ertürk A, Becker K, Jährling N et al (2012) Three-dimensional imaging of solvent-cleared organs using 3DISCO. Nat Protoc 7(11):1983–1995

Frye MD, Yang W, Zhang C, Xiong B, Hu BH (2017) Dynamic activation of basilar membrane macrophages in response to chronic sensory cell degeneration in aging mouse cochleae. Hear Res 344:125–134. https://doi.org/10.1016/j.heares.2016.11.003

Fujimoto C, Iwasaki S, Urata S et al (2017) Autophagy is essential for hearing in mice. Cell Death Dis 8(5):e2780. https://doi.org/10.1038/cddis.2017.194

Fujioka M, Okano H, Ogawa K (2014) Inflammatory and immune responses in the cochlea: potential therapeutic targets for sensorineural hearing loss. Front Pharmacol 5. https://www.frontiersin.org/articles/https://doi.org/10.3389/fphar.2014.00287

Greenbaum A, Chan KY, Dobreva T et al (2017) Bone CLARITY: clearing, imaging, and computational analysis of osteoprogenitors within intact bone marrow. Sci Transl Med. 9(387):eaah6518

Hama H, Kurokawa H, Kawano H et al (2011) Scale: a chemical approach for fluorescence imaging and reconstruction of transparent mouse brain. Nat Neurosci 14(11):1481–1488

Hirose K, Discolo CM, Keasler JR, Ransohoff R (2005) Mononuclear phagocytes migrate into the murine cochlea after acoustic trauma. J Comp Neurol 489(2):180–194

Hough K, Verschuur CA, Cunningham C, Newman TA (2022) Macrophages in the cochlea; an immunological link between risk factors and progressive hearing loss. Glia 70(2):219–238. https://doi.org/10.1002/glia.24095

Hutson KA, Pulver SH, Ariel P, Naso C, Fitzpatrick DC (2021) Light sheet microscopy of the gerbil cochlea. J Comp Neurol 529(4):757–785. https://doi.org/10.1002/cne.24977

Jiang H, Wang X, Zhang J, Kachelmeier A, Lopez IA, Shi X (2019) Microvascular networks in the area of the auditory peripheral nervous system. Hear Res 371:105–116. https://doi.org/10.1016/j.heares.2018.11.012

Kakigi A, Egami N, Uehara N et al (2020) Live imaging and functional changes of the inner ear in an animal model of Meniere's disease. Sci Rep 10(1):1–10

Keppeler D, Kampshoff CA, Thirumalai A et al (2021) Multiscale photonic imaging of the native and implanted cochlea. Proc Natl Acad Sci 118(18):e2014472118. https://doi.org/10.1073/pnas.2014472118

Kikuchi T, Kimura RS, Paul DL, Adams JC (1995) Gap junctions in the rat cochlea: immunohistochemical and ultrastructural analysis. Anat Embryol (berl) 191(2):101–118. https://doi.org/10.1007/BF00186783

Kim J, Ricci AJ (2022) In vivo real-time imaging reveals megalin as the aminoglycoside gentamicin transporter into cochlea whose inhibition is otoprotective. Proc Natl Acad Sci 119(9):e2117946119. https://doi.org/10.1073/pnas.2117946119

Liu W, Danckwardt-Lillieström N, Schrott-Fischer A, Glueckert R, Rask-Andersen H (2021) Distribution of immune cells including macrophages in the human cochlea. Front Neurol. https://www.frontiersin.org/articles/https://doi.org/10.3389/fneur.2021.781702

Lugo-Hernandez E, Squire A, Hagemann N et al (2017) 3D visualization and quantification of microvessels in the whole ischemic mouse brain using solvent-based clearing and light sheet microscopy. J Cereb Blood Flow Metab 37(10):3355–3367. https://doi.org/10.1177/0271678X17698970

MacDonald GH, Rubel EW (2008) Three-dimensional imaging of the intact mouse cochlea by fluorescent laser scanning confocal microscopy. Hear Res 243(1–2):1–10. https://doi.org/10.1016/j.heares.2008.05.009

MacDonald GH, Rubel EW (2010) Three-dimensional confocal microscopy of the mammalian inner ear. Audiol Med 8(3):120–128. https://doi.org/10.3109/1651386X.2010.502301

Malfeld K, Armbrecht N, Volk HA, Lenarz T, Scheper V (2021) In situ 3D-imaging of the inner ear synapses with a cochlear implant. Life. https://doi.org/10.3390/life11040301

Mizushima Y, Fujimoto C, Kashio A, Kondo K, Yamasoba T (2017) Macrophage recruitment, but not interleukin 1 beta activation, enhances noise-induced hearing damage. Biochem Biophys Res Commun 493(2):894–900. https://doi.org/10.1016/j.bbrc.2017.09.124

Moatti A, Cai Y, Li C et al (2020) Three-dimensional imaging of intact porcine cochlea using tissue clearing and custom-built light-sheet microscopy. Biomed Opt Express 11(11):6181–6196

Moatti A, Li C, Sivadanam S et al (2022) Ontogeny of cellular organization and LGR5 expression in porcine cochlea revealed using tissue clearing and 3D imaging. Iscience 25(8):104695

Murakami TC, Mano T, Saikawa S et al (2018) A three-dimensional single-cell-resolution whole-brain atlas using CUBIC-X expansion microscopy and tissue clearing. Nat Neurosci 21(4):625–637

Neng L, Zhang F, Kachelmeier A, Shi X (2013) Endothelial Cell, pericyte, and perivascular resident macrophage-type melanocyte interactions regulate cochlear intrastrial fluid-blood barrier permeability. J Assoc Res Otolaryngol 14(2):175–185. https://doi.org/10.1007/s10162-012-0365-9

Nin F, Hibino H, Doi K, Suzuki T, Hisa Y, Kurachi Y (2008) The endocochlear potential depends on two K+ diffusion potentials and an electrical barrier in the stria vascularis of the inner ear. Proc Natl Acad Sci 105(5):1751–1756. https://doi.org/10.1073/pnas.0711463105

Niyazov DM, Andrews JC, Strelioff D, Sinha S, Lufkin R (2001) Diagnosis of endolymphatic hydrops in vivo with magnetic resonance imaging. Otol Neurotol 22(6). https://journals.lww.com/otology-neurotology/Fulltext/2001/11000/Diagnosis_of_Endolymphatic_Hydrops_In_Vivo_with.17.aspx

Nolte L, Tinne N, Schulze J et al (2017) Scanning laser optical tomography for in toto imaging of the murine cochlea. PLoS ONE 12(4):e0175431. https://doi.org/10.1371/journal.pone.0175431

Nomura Y, Hiraide F (1968) Cochlear blood vessel: a histochemical method of its demonstration. Arch Otolaryngol 88(3):231–237. https://doi.org/10.1001/archotol.1968.00770010233004

Nwaneshiudu A, Kuschal C, Sakamoto FH, Anderson RR, Schwarzenberger K, Young RC (2012) Introduction to confocal microscopy. J Invest Dermatol 132(12):1–5

Pan C, Cai R, Quacquarelli FP et al (2016) Shrinkage-mediated imaging of entire organs and organisms using uDISCO. Nat Methods 13(10):859–867

Risoud M, Sircoglou J, Dedieu G, Tardivel M, Vincent C, Bonne N-X (2017) Imaging and cell count in cleared intact cochlea in the Mongolian gerbil using laser scanning confocal microscopy. Eur Ann Otorhinolaryngol Head Neck Dis 134(4):221–224. https://doi.org/10.1016/j.anorl.2017.01.001

Sautter NB, Shick EH, Ransohoff RM, Charo IF, Hirose K (2006) CC Chemokine receptor 2 is protective against noise-induced hair cell death: studies in CX3CR1+/GFP mice. J Assoc Res Otolaryngol 7(4):361–372. https://doi.org/10.1007/s10162-006-0051-x

Shi X (2010) Resident macrophages in the cochlear blood-labyrinth barrier and their renewal via migration of bone-marrow-derived cells. Cell Tissue Res 342(1):21–30. https://doi.org/10.1007/s00441-010-1040-2

Steffen J, Julio A, Petra G et al (2000) Analysis of fractalkine receptor CX3CR1 function by targeted deletion and green fluorescent protein reporter gene insertion. Mol Cell Biol 20(11):4106–4114. https://doi.org/10.1128/MCB.20.11.4106-4114.2000

Susaki EA, Tainaka K, Perrin D et al (2014) Whole-brain imaging with single-cell resolution using chemical cocktails and computational analysis. Cell 157(3):726–739

Susaki EA, Tainaka K, Perrin D, Yukinaga H, Kuno A, Ueda HR (2015) Advanced CUBIC protocols for whole-brain and whole-body clearing and imaging. Nat Protoc 10(11):1709–1727. https://doi.org/10.1038/nprot.2015.085

Tasaki I, Spyropoulos CS (1959) Stria vascularis as source of endocochlear potential. J Neurophysiol 22(2):149–155

Tinne N, Antonopoulos GC, Mohebbi S et al (2017) Three-dimensional hard and soft tissue imaging of the human cochlea by scanning laser optical tomography (SLOT). PLoS ONE 12(9):e0184069. https://doi.org/10.1371/journal.pone.0184069

Todorov MI, Paetzold JC, Schoppe O et al (2020) Machine learning analysis of whole mouse brain vasculature. Nat Methods 17(4):442–449. https://doi.org/10.1038/s41592-020-0792-1

Toulemonde P, Risoud M, Lemesre PE, Tardivel M, Siepmann J, Vincent C (2022) 3D analysis of gerbil cochlea with cochlear implant. Eur Ann Otorhinolaryngol Head Neck Dis. https://doi.org/10.1016/j.anorl.2022.03.002

Urata S, Iida T, Suzuki Y et al (2019a) A novel technique for imaging and analysis of hair cells in the organ of Corti using modified Sca/eS and machine learning. Bio-Protoc 9(16):e3342–e3342

Urata S, Iida T, Yamamoto M et al (2019b) Cellular cartography of the organ of Corti based on optical tissue clearing and machine learning. Elife. https://doi.org/10.7554/eLife.40946

Wang Q, Liu K, Yang L, Wang H, Yang J (2019) BoneClear: whole-tissue immunolabeling of the intact mouse bones for 3D imaging of neural anatomy and pathology. Cell Res 29(10):870–872

Wrzeszcz A, Reuter G, Nolte I, Lenarz T, Scheper V (2013) Spiral ganglion neuron quantification in the guinea pig cochlea using confocal laser scanning microscopy compared to embedding methods. Hear Res 306:145–155. https://doi.org/10.1016/j.heares.2013.08.002

Zhang W, Dai M, Fridberger A et al (2012) Perivascular-resident macrophage-like melanocytes in the inner ear are essential for the integrity of the intrastrial fluid-blood barrier. Proc Natl Acad Sci U S A 109(26):10388–10393. https://doi.org/10.1073/pnas.1205210109